ELSEVIER

Cement & Concrete Composites 25 (2003) 617–623

Cement & Concrete Composites

www.elsevier.com/locate/cemconcomp

Biaxial tension fatigue response of concrete

Kolluru V. Subramaniam *, Surendra P. Shah

Civil Engineering Department, T-110 Steinman Hall, City College of New York, Convent Avenue at 140th Street, New York, NY 10031, USA

Abstract

Concrete structures such as rigid airport pavements are subjected to repeated high-amplitude loads resulting from passing aircraft. The resulting stress-state in concrete is a biaxial combination of compression and tension. It is of interest to understand the response of plain concrete to such loading conditions, which will enable development of realistic material models for implementation in mechanistic pavement design procedures.

The objective of this work is to characterize the quasi-static and low-cycle fatigue response of concrete subjected to biaxial stresses in the biaxial tension region, where the principal tensile stress is larger than or equal in magnitude when compared with the principal compressive stress. An experimental investigation of material behavior in the biaxial tension region is conducted. The experimental setup consists of the following test configurations: (a) notched concrete beams tested in three-point bend configuration, and (b) hollow concrete cylinders subjected to torsion.

Failure of concrete in the biaxial tension region is shown to be a local phenomenon under quasi-static and fatigue loading, wherein the specimen fails owing to a single crack. The crack propagation is studied using the equivalent elastic crack concept. It is observed that the crack growth rate in constant amplitude fatigue loading exhibits a two-phase process: a deceleration phase followed by an acceleration stage. The crack growth in the acceleration stage is shown to follow Paris law. The model parameters obtained from uniaxial fatigue tests are shown to be sufficient for predicting the considered biaxial fatigue response.

Keywords: Fatigue; Concrete; Biaxial; Fracture; Paris law; High-amplitude; Tension; Torsion

1. Background

Fatigue is the process of progressive, localized and permanent material damage. A distinction is generally made between low-cycle, high-amplitude fatigue and high-cycle, low-amplitude fatigue. The former involves few load cycles of high stress (earthquakes, storms, etc.) while the latter is characterized by a greater number of cycles of low stress (wind and wave loading). While at low stress amplitudes, the cycling causes progressive degradation of material stiffness and often leads to sudden failures with little or no plastic deformation, repeated cycling at high stress level where the response of the material is non-linear causes severe damage in a relatively small number of cycles. A comprehensive review of the fatigue behavior of concrete is provided in committee reports of RILEM and American Concrete Institute (ACI) [1,4,8]. Most of the results reported in the literature pertain to uniaxial loading (tension and compression).

Very few experimental results on the response of concrete subjected to repeated biaxial loading are available in the literature. All the results in the literature pertain to cyclic biaxial compression, where both principal stresses are compressive [3,7,11]. From their experimental investigation considering four different principal stress ratios, Su and Hsu [11] established that the S–N relationship for concrete subjected to biaxial compression was curved instead of being a straight line. Su and Hsu [11] idealized the observed S–N curve by two straight lines and the slope for the low-cycle fatigue was seen to be several times higher than that for high cycle fatigue. Further, the fatigue strength of concrete for biaxial compression was shown to be greater than that for uniaxial compression for any given number of cycles [11]. Visual observation of the failed specimens

* Corresponding author. Fax: +1-212-650-6965.
E-mail address: ksubram@ce.ccny.cuny.edu (K.V. Subramaniam).

0958-9465/02/$ - see front matter © 2002 Elsevier Science Ltd. All rights reserved.
doi:10.1016/S0958-9465(02)00075-6

indicated that the failure mode under quasi-static and fatigue loadings was identical. The S–N relationship was also observed to be a curve in the case of high strength concrete [7]. No reference concerning the behavior of concrete subjected to fatigue loading in the biaxial tension region was found in the literature. In addition, an understanding of the propagation of damage in concrete subjected to repeated biaxial tension stresses, based on physical principles could not be found.

2. Introduction

In this paper the quasi-static and fatigue behavior of concrete is investigated in the biaxial stress space where the magnitude of the principal tensile stress is larger than or equal to the magnitude of the principal compressive stress and is referred to as the biaxial tension region. In particular, the damage mechanism and the propagation of damage in quasi-static and high-amplitude fatigue are studied. The biaxial stress region of interest, the biaxial tension region, is bounded by pure tension at one end and the state of equal compression–tension at the other end (Fig. 1). In the experimental program two different test configurations were used. Concrete beam specimens were tested in a three-point bend configuration to obtain the uniaxial tensile material properties. The experimental setup for generating biaxial stresses consisted of applying torsional loading to hollow cylindrical concrete specimens. Torsion introduces a state of pure shear stress in the material which, when resolved in terms of principal stresses corresponds to a biaxial state of stress wherein the two principal stresses are equal in magnitude but of opposite signs. The ratio of the two principal stresses remains constant during the entire loading procedure. The ratio of the two principal stresses can be changed by superposition of an axial load over the torsional load. The entire biaxial region between the limits corresponding to uniaxial tension and compression can be spanned by varying the magnitude of the applied axial load. This process is illustrated schematically in Fig. 1.

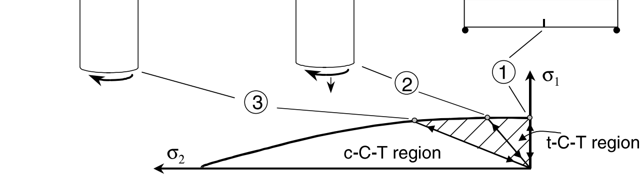

Fig. 1. Schematic representation of the test configurations in the biaxial tension stress-state.

3. Failure mechanism in biaxial tension region

When a concrete structure is subjected to an external tensile loading, microcracks occur at the cement-aggregate interfaces or at any defects present in the concrete. As the load starts increasing some of the microcracks grow and eventually several of these microcracks will coalesce to form a macro-crack [6]. The macro-crack propagates in a stable manner until the critical load is reached. For structures, of positive geometry (where the stress intensity factor increases with an increase in crack length), the critical load corresponds with the peak load. The crack propagates in an unstable manner after the peak load. The formation and propagation of the single crack dominates the complete load history of such structures.

Through carefully controlled experimentation it was shown that that the torque-rotation response of hollow concrete cylinders also exhibits a region of stable crack growth that is followed by a softening response owing to propagation of a single crack in the gage region [12]. The crack was found to initiate in the pre-peak part of the load response and the post-peak part of the load response was governed by the crack propagation. Experimental evidence indicated that the decrease in rotational stiffness of the specimen during a fatigue test was a result of propagation of a single crack. To understand the material response to shear loading, it is hence important to obtain information about the crack growth resulting from torsional loading of the specimen. The problem can then be studied using fracture mechanics, and a fracture-based crack growth criterion can be established for such loading. The evolution of damage under fatigue loading can then be studied and a fracture-based fatigue damage law can be developed.

4. Crack growth in concrete

Owing to effects such as tortuous crack path, and difficulty in determining the crack tip due to particles bridging the crack, the true crack length cannot be measured directly in concrete structures [10, p. 113]. The crack length is instead estimated indirectly from the measured increase in the compliance of the specimen. The increase in compliance of a specimen is attributed to the propagation of a single *effective crack* in an elastic medium, and is referred to as the equivalent elastic crack concept. The effective crack is a traction free crack that gives the same compliance as the true crack. Crack growth in the concrete structure is then studied in terms of this effective traction free crack and principles of LEFM are applied to study propagation of the effective crack [5].

4.1. Compliance calibration

Closed form solution that relates the compliance of a beam subjected to three-point bend configuration with the crack length is available. For a notched beam specimen tested in three-point bend configuration, Young's modulus (E) of the material is calculated as

$$E = \frac{6Sa_0V_1(\alpha)}{C_i bd^2} \quad \text{where}$$
$$V_1(\alpha) = 0.76 - 2.26\alpha + 3.87\alpha^2 - 2.04\alpha^3 + \frac{0.66}{(1-\alpha)^2} \tag{1}$$

C_i is the initial compliance (inverse of the slope) calculated from the load-crack mouth opening displacement curve, a_0 the initial notch length, S the span of the beam, b and d are the thickness and depth of the beam, respectively and $\alpha = a_0/d$. The effective crack length, a_e, at any point in the load response of the beam can be now computed from the unloading compliance, C_u, obtained by unloading the specimen at different points on the quasi-static load envelope. Using an iterative process, a_e is found when Eq. (2) is satisfied

$$E = \frac{6Sa_eV_1(\alpha)}{C_u bd^2} \tag{2}$$

where $\alpha = a_e/d$. This procedure for computing the effective crack length for a notched beam subjected to three-point bending configuration was established by Jenq and Shah [5] and subsequently became a RILEM recommendation [9].

The effective crack length in a cylinder subjected to torsion can also be similarly estimated from the change in rotational compliance (inverse of stiffness) of the specimen. This is known as the compliance calibration of the equivalent crack length and the concept was first demonstrated for concrete specimens by Swartz et al. [16]. It is based on the property that in LEFM the displacements are proportional to the load, and the associated compliance is uniquely related to the crack length. Unfortunately, closed-form solutions for prediction of the compliance as a function of crack length are not available for this particular specimen geometry. A numerical analysis was performed to predict the crack length from the compliance measurements. In this analysis it was implicitly assumed that the decrease in rotational stiffness (increase in rotational compliance) is a result of the propagation of a single effective crack. The actual crack was modeled in terms of an effective crack embedded in an elastic material matrix. The values of E and v for concrete used in the numerical analysis were 33.67 and 0.187 GPa, respectively. Details of the numerical analysis are presented by Subramaniam [14].

Numerical analyses were performed for a cylinder with cracks of different lengths to determine the influence of crack length on the rotational stiffness (inverse of compliance) and the stress intensity factors at the crack tip. The analysis was performed using the boundary element solver available within the FRANC3D™ program. Through numerical analysis it was also established that the crack propagation is governed by the K_I stress intensity factor at the crack tip, under such loading [14]. Fig. 2 shows a plot of the computed change in rotational stiffness of the specimen for different assumed crack lengths; the solid line shows the computed stiffness change, which takes the form a polynomial. Cylinders were also cast with pre-placed through-thickness notches of different lengths. The triangles in Fig. 2 show the measured rotational stiffness of these specimens determined through mechanical tests. The percentage change in the rotational stiffness has been computed with respect to the rotational stiffness for the uncracked (pristine) specimen. It can be seen that results of the numerical simulation corresponds well with the experimentally obtained values of the rotational stiffness of cylinder with notches of different lengths. The effective crack length can now be determined from the decrease in rotational stiffness using the results in Fig. 2. The change in compliance of the specimen under

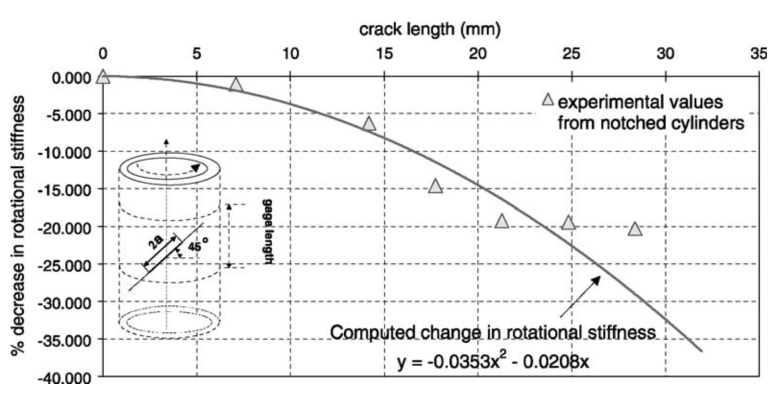

Fig. 2. Decrease in rotational stiffness (increase in compliance) of the hollow cylinder with simulated through-thickness cracks of different lengths (line) and actual cracks (triangular points).

quasi-static and fatigue loadings can now be studied using the concept of effective crack assuming that the decrease in stiffness (increase in compliance) is caused by the propagation of this effective crack.

5. Crack growth in biaxial tension region

5.1. Quasi-static loading

The quasi-static load response in the biaxial tension region was observed to exhibit softening response in the post-peak that was attributed to crack growth [12]. The quasi-static response may be framed in terms of fracture parameters and visualized as a failure envelope curve in terms of crack length, where each point in the post-peak region is an equilibrium point representing the maximum load that can be supported for that given crack length. Following the procedure previously established by Jenq and Shah [5], an estimation of the effective crack length can be obtained by unloading the specimen from the static envelope curve. A typical cyclic quasi-static response of a hollow cylinder subjected to torsion, obtained by unloading the specimen at different points in the post-peak part of the load response and then reloading is shown in Fig. 3. There is a progressive decrease in the structural stiffness (increase in compliance) due to crack propagation as evidenced by the decrease in the slope of the loading–unloading curves in the post-peak. The change in compliance of the specimen is ascribed to the propagation of an effective crack and the crack length at different points in the post-peak response is obtained using the compliance calibration curve developed in the previous section.

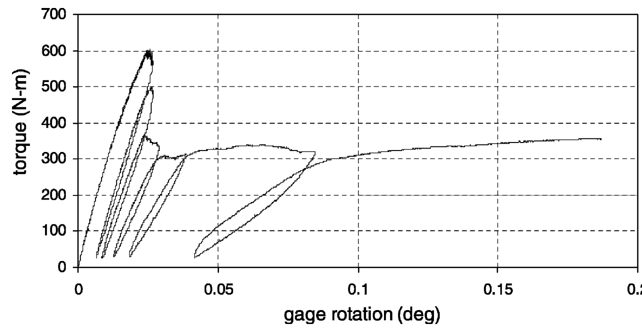

Fig. 3. Typical quasi-static cyclic torsional response obtained by unloading the specimen at different points in the post-peak part of the torsional response.

5.2. Fatigue loading

Constant amplitude, fatigue tests were conducted in both flexure and torsion at three different load ranges [13,15]. In all the fatigue tests, the lower load level in a fatigue load cycle was kept constant, equal to 5% of the average quasi-static peak load. Three different upper load levels corresponding to 75%, 85%, and 90% of the average quasi-static peak load were used in the study. The crack length during fatigue loading was determined from the observed change in compliance of the specimen using the compliance calibration curve. A typical fatigue crack growth curve for a specimen where the upper load level was equal to 85% of the average quasi-static peak load is shown in Fig. 4. The number of fatigue cycles for this particular specimen has been normalized with respect to the number of cycles to failure (N_f) in Fig. 4(a) to show clearly the observed response as a function of the relative fatigue life of the specimen. Similar response was also observed in all specimens tested in flexure and

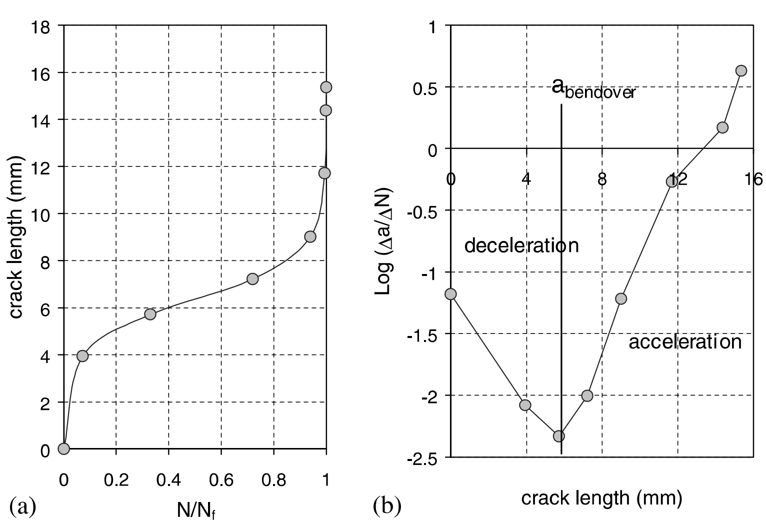

Fig. 4. Crack growth during torsional fatigue loading (a) crack length versus normalized number of cycles and (b) rate of crack growth versus crack length.

at all the load ranges. It is observed that the rate of crack growth exhibits an initial deceleration that is followed by an acceleration stage up to failure. The crack length where the rate of fatigue crack growth changes from deceleration to acceleration has been labeled $a_{bendover}$. $a_{bendover}$ corresponds to the crack length at the inflection point in the crack length versus number of cycles plot. Any understanding of this two-stage response of fatigue crack growth requires a fundamental understanding of the mechanisms that influence crack growth in concrete. Detailed listing showing the statistical variation in N_f and other measured parameters are provided in [14].

5.3. Mechanisms that influence crack growth

In concrete, as the crack grows the fracture process zone that represents the inelastic zone around the crack increases in size. The growth of the fracture process zone is associated with an increase in the resistance (energy required for unit crack extension) to crack growth. As the crack starts to grow, further crack growth requires larger energy because of the increase in the fracture process zone. As the crack grows there is also an increase in the driving force provided by the increasing stress intensity factor at the crack tip. Crack growth in concrete structures is hence influenced by two competing mechanisms. As the crack starts to grow from a notch or a flaw, the growth of the fracture process zone and the energy absorbed by it ensure stable crack growth (crack grows only when the applied load is increased) until the crack reaches a critical crack length ($a_{critical}$). The critical crack length corresponds with the peak load of the structure under quasi-static loading [2]. After peak load the resistance to crack growth has been shown to attain a constant value [2]. The increasing crack growth resistance and crack driving force are functions of both geometry and material.

The process of crack growth under constant amplitude fatigue loading also experiences the influence of increasing crack growth resistance and crack driving force. The process of fatigue crack growth is illustrated schematically in Fig. 5. As the crack grows the crack driving force is provided by the increasing stress intensity factor at the crack tip (Fig. 5(b)). Simultaneously there is also an increase in the resistance to crack growth provided by the increase in the inelastic fracture process zone (Fig. 5(a)). While the crack driving force is a monotonically increasing function of crack length, the crack resistance eventually attains a steady state value [2].

Under quasi-static loading, the fracture resistance attains a constant value at $a_{critical}$, which corresponds to the peak load. Therefore it can be hypothesized that the crack length where the rate of fatigue crack growth changes from deceleration to acceleration ($a_{bendover}$) corresponds with the fracture resistance attaining a constant value. A comparison of the critical crack length at the peak load of the quasi-static response ($a_{critical}$) and the crack length at the bendover point, where the rate of crack growth changes from deceleration to acceleration ($a_{bendover}$) is shown in Fig. 6(a) and (b) for flexure and torsion specimens, respectively. Each point on the graph corresponds to one specimen tested in fatigue. The *X*-axis corresponds to the maximum applied load in a fatigue–load cycle as a percentage of the average maximum quasi-static peak load. The *Y*-axis of the graph is the ratio of $a_{bendover}$ to the average $a_{critical}$ obtained by testing six specimens under cyclic quasi-static loading. From the figure it can be seen that while there is some scatter, $a_{bendover}$ in the fatigue response at load ranges used in this study is the same magnitude as $a_{critical}$ of the quasi-static monotonic response. Therefore for high amplitude fatigue loading such as that considered in this study, $a_{bendover}$ in the fatigue response can be considered equal to $a_{critical}$ that is obtained from the quasi-static response.

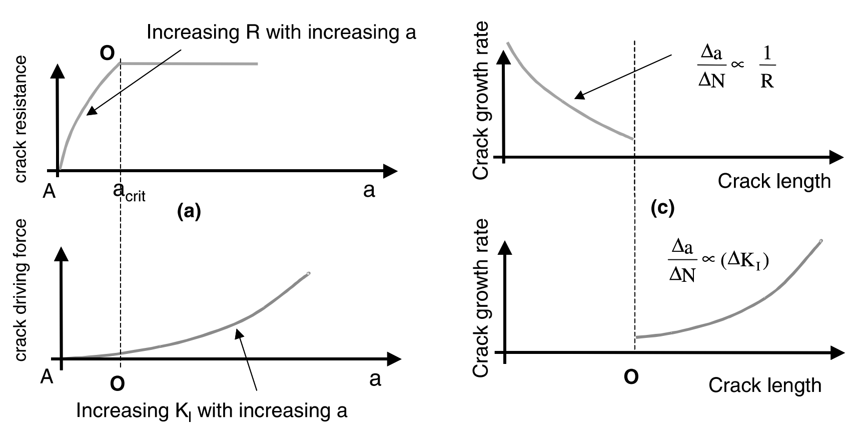

Fig. 5. The mechanisms that influence the crack growth (a) increasing resistance and (b) crack driving force with crack growth. The mechanistic model for fatigue crack growth (c) during deceleration stage and (d) during acceleration stage.

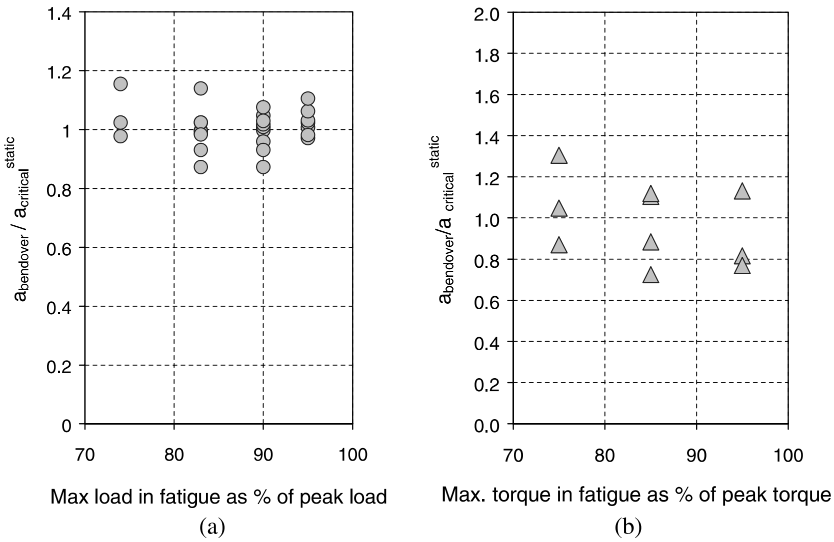

Fig. 6. Comparison of a_{bendover} in fatigue and a_{critical} in quasi-static loading in (a) flexure and (b) torsion.

5.4. Analytical model

The authors [15] recently proposed a simplified model for fatigue crack growth under uniaxial loading. In the deceleration stage, increasing K_I with increasing crack has a minor influence. This effect is ignored in this simplified model. In the deceleration stage, the reduction in the crack growth rate per unit crack advance is assumed to be proportional to the increasing resistance (rising *R*-curve) experienced by the crack (Fig. 5(c)). The resistance is proportional to the total increase in crack length from the beginning of loading ($Da = a - a_0$). It is proposed that the rate of crack growth in this stage can be represented by the expression

$$\frac{\Delta a}{\Delta N} = C_1 (Da)^{n_1} \tag{3}$$

where C_1 and n_1 are the constant and the exponent respectively, to be determined from the experimental data. Justification for the chosen form is provided by Subramaniam et al. [15].

In the acceleration stage, it is assumed that the crack growth rate can be predicted by Paris law given below

$$\frac{\Delta a}{\Delta N} = C_2 (\Delta K_I)^{n_2} \tag{4}$$

where C_2 and n_2 are the constant and exponent of the Paris law respectively, to be determined from the experimental data (Fig. 5(d)).

The fatigue coefficients were obtained from the flexural fatigue tests. Average values of $\text{Log}(C_1)$ and n_1 were determined to be −2.05 and −1.7, respectively, when the stress amplitude is below 90% of the quasi-static value, while the average values of the coefficients were −0.65 and −1.25, respectively, when the stress amplitude was greater than 90% [15]. In addition, using flexural fatigue data the coefficients $\text{Log}(C_2)$ and n_2 were determined to be −28.66 and 17.33 for all the load ranges [15]. Data and detailed analysis of the results for

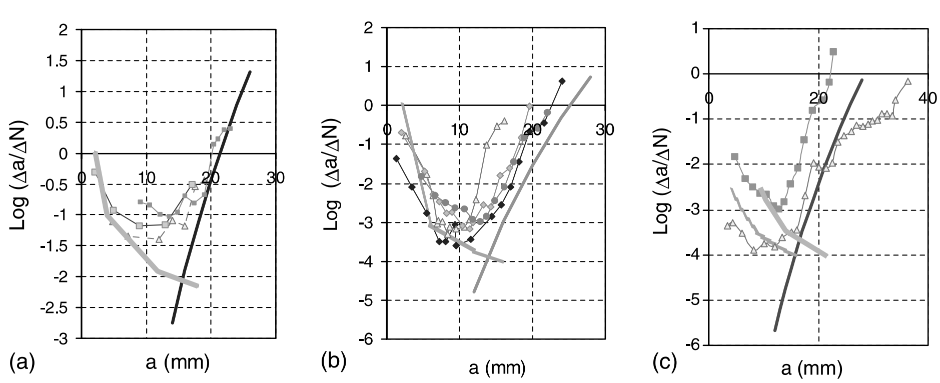

Fig. 7. Comparison between analytical prediction (grey line: deceleration; black line: acceleration) and experimental data: maximum fatigue torque equal to (a) 95%, (b) 85% and (c) 75% of the peak quasi-static torque. Each symbol-type in the three graphs corresponds to one specimen tested in fatigue.

all the load ranges tested in both torsion and flexure are given in [14]. A comparison of the experimental data from the torsion fatigue tests and the model predictions for the deceleration and the acceleration stages using the fatigue coefficients obtained from flexure are shown in Fig. 7. There is a good match between the experimental data and the model predictions; fatigue coefficients from flexure predict the fatigue crack growth in torsion reasonably well. Since the stress states that correspond to torsion and flexure represent the two boundaries of the biaxial tension region, it can be postulated that the fatigue crack growth in this biaxial region (for proportional loading) can be predicted using the uniaxial tensile material parameters.

6. Conclusions

Based on the results presented in this paper, the following conclusions are drawn:

(1) There are two competing mechanisms that influence the crack growth rate during constant amplitude fatigue loading: (a) increasing resistance to crack growth, and (b) increasing K_I with crack length that accelerates the crack growth. The crack length at which the rate of fatigue crack growth changes from deceleration to acceleration is of the same magnitude as the crack length at the peak load in the quasi-static response.
(2) The crack growth in the acceleration stage can be accurately modeled using Paris law. The Paris coefficients can be considered to be material constants for high amplitude fatigue loading.
(3) The material constants obtained from flexural fatigue can be used to predict the fatigue crack propagation in biaxial tension region sufficiently accurately using the simplified physically based model for crack growth presented in this paper.

References

[1] ACI Committee 215, In: Shah SP, editor. Fatigue of concrete structures. Publication SP-75. Detroit: American Concrete Institute; 1982.
[2] Bazant ZP, Planas J. Fracture and size effect in concrete and other quasi-brittle materials. Boca Raton: CRC Press; 1998.
[3] Buyukozturk O, Tseng T. Concrete in biaxial compression. J Struct Eng (ASCE) 1984;110(3):461–76.
[4] Hawkins NM, Shah SP. American concrete institute considerations for fatigue. In: IABSE colloqium, Fatigue of steel and concrete structures, Lousanne, Proceedings IABSE reports, Zurich, vol. 37. 1982, p. 41–50.
[5] Jenq YS, Shah SP. Fracture toughness criterion for concrete. Eng Fract Mech 1985;21:1055–69.
[6] Li Z, Shah SP. Localization of microcracking under uniaxial tension. ACI Mater J 1994;91(4).
[7] Nelson EL, Carrasquillo RL, Fowler DW. Behavior and failure of high-strength concrete subjected to biaxial-cyclic compression loading. ACI Mater J 1988:248–53.
[8] RILEM Committee 36-RDL. Long term random dynamic loading of concrete structures, RILEM Mater Struct 1984;17(97):1–28.
[9] RILEM. Determination of fracture parameters (K_{IC}^S and $CTOD_c$) of plain concrete using three-point bend tests. Mater Struct 1990;23:457–460 [RILEM draft recommendation, TC 89-FMT fracture mechanics of concrete—test methods].
[10] Shah SP, Swartz SE, Ouyang C. Fracture mechanics of concrete. New York: Wiley Intersciense; 1995.
[11] Su ECM, Hsu TTC. Biaxial compression fatigue and discontinuity of concrete. ACI Mater J 1988:178–88.
[12] Subramaniam KV, Popovics JS, Shah SP. Testing concrete in torsion: instability analysis and experiments. J Eng Mech, Am Soc Civ Eng (ASCE) 1998;124(11):1258–68.
[13] Subramaniam KV, Popovics JS, Shah SP. Fatigue behavior of concrete subjected to biaxial stresses in the C–T region. Mater J, Am Concr Inst (ACI) 1999;96(6):663–9.
[14] Subramaniam KV. Fatigue of concrete subjected to biaxial loading in the tension region, Ph.D. Dissertation, Northwestern University, 1999b.
[15] Subramaniam KV, Popovics JS, Shah SP. Flexural fatigue of concrete: experiments and theoretical model. J Eng Mech, Am Soc Civ Eng (ASCE) 2000;126(9):891–8.
[16] Swartz SE, Hu KK, Jones GL. Compliance monitoring of crack growth in concrete. J Eng Mech (ASCE) 1978;104:789–800.